Expanded View Figures

Figure EV1. Prolonged NF-κB activation in astrocytes induces microglia differentiation.

A, B Co-immunostaining of CD11b, TMEM119, DAPI, and quantification of $CD11b^+/TMEM119^+$ and $CD11b^+/TMEM119^-$ cells in SOD1/IKK mice; more than 90% of $CD11b^+$ cells are $TMEM119^+$, confirming the microglial identity.

C, D Immunostaining for microglia (IBA1), macrophages (F4/80), DAPI, and quantification of $F4/80^+/IBA1^+$ cells. $F4/80^+$ cells represent only a very small percentage of $IBA1^+$ cells.

E, F Co-immunostaining of TMEM119, CD45, DAPI, and quantification of $TMEM119^+/CD45^+$; CD45 identifies a subset of $TMEM119^+$ microglia.

G, H Immunostaining for MAC-2, CD45, DAPI, and the relative quantification of $CD45^+/MAC\text{-}2^+$ and $CD45^+/MAC\text{-}2^-$ fraction; only a subset of $CD45^+$ cells are also $MAC\text{-}2^+$.

I, J Immunostaining of CD11b, MAC-2, DAPI, and quantification of $CD11b^+/MAC\text{-}2^+$ fraction, confirming that $MAC\text{-}2^+$ cells represent a subset of microglia.

K Schematic summary of cell identity according to immunohistochemistry in Figs 2 and EV1.

L, M Co-immunostaining of CD11b, CD11c, DAPI, and quantification of $CD11b^+/CD11c^+$ (DAM) fraction; $CD11c^+$ cells represent about 25% of myeloid cells.

N, O Immunostaining of TMEM119, CD11c, DAPI, and quantification of $CD11c^+/TMEM119^+$, showing that nearly all $CD11c^+$ are microglia and not infiltrating cells.

P–R Immunostaining of TMEM119, CD11c, CD169, and quantification of $TMEM119^+/CD11c^+$ fraction expressing the monocyte marker CD169; almost no $CD11c^+$ cell is $CD169^+$, confirming that $CD11c^+$ are not infiltrating monocytes; nevertheless, a distinct population of $TMEM119^+/CD169^+$ early-activated microglia can be identified (R).

S Time course of $CD11c^+$ cell fraction in the overall $CD11b^+$ population; the DAM population does not expand in the progression phase.

Data information: Representative images are shown only for SOD1/IKK. Quantification is shown for both SOD1/IKK ($n = 3$) and IKK ($n = 3$) at P50. In (A, C, E, G, I, L and N), the bottom panels represent the high-magnified views of the upper panels. Data are presented as means ± SD. Scale bars, 10 μm.

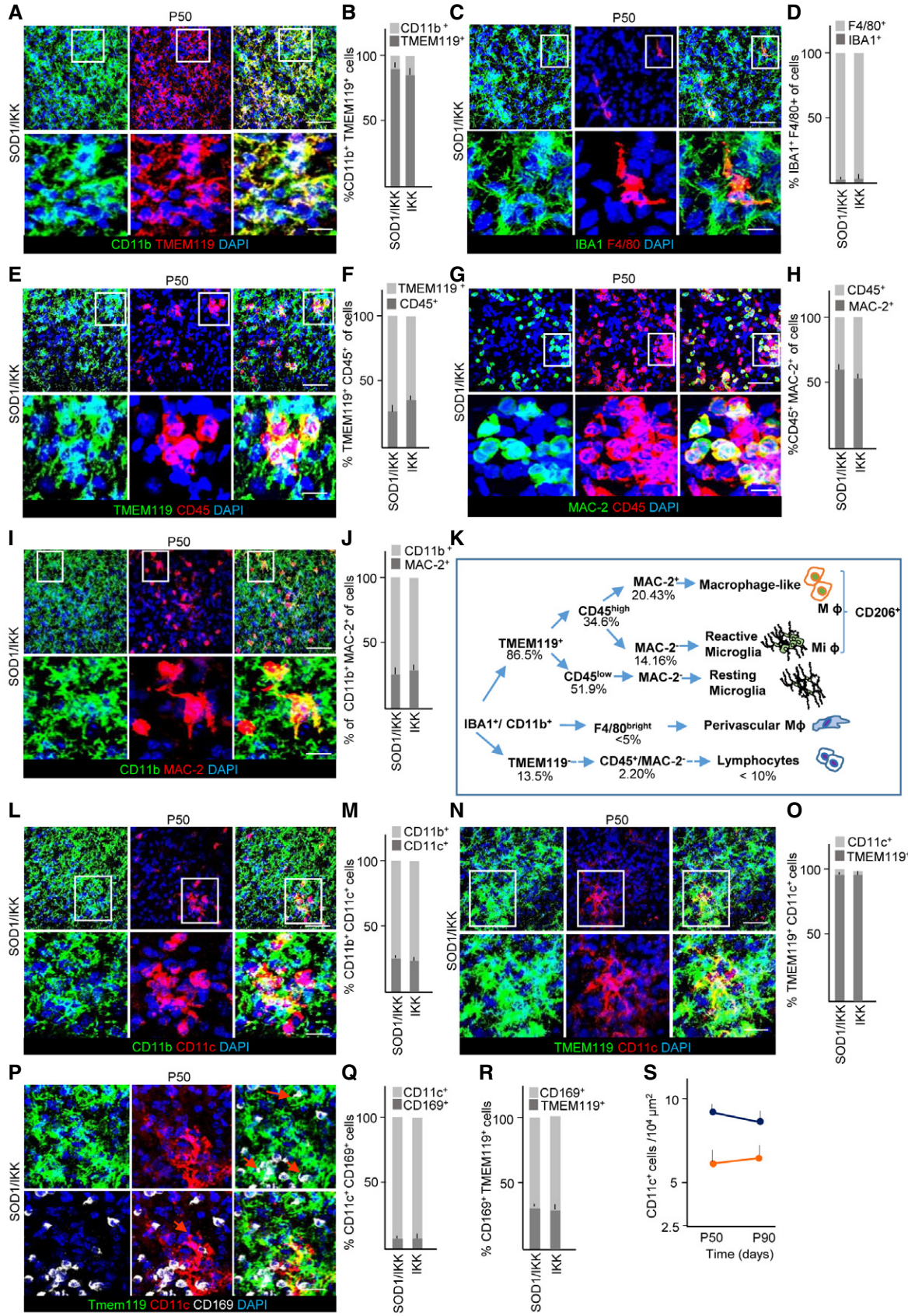
A
P50
SOD1/IKK
CD11b TMEM119 DAPI
B
CD11b+
TMEM119+
%CD11b+ TMEM119+ cells
SOD1/IKK
IKK
C
P50
SOD1/IKK
IBA1 F4/80 DAPI
D
F4/80+
IBA1+
% IBA1+ F4/80+ of cells
SOD1/IKK
IKK
E
P50
SOD1/IKK
TMEM119 CD45 DAPI
F
TMEM119+
CD45+
% TMEM119+ CD45+ of cells
SOD1/IKK
IKK
G
P50
SOD1/IKK
MAC-2 CD45 DAPI
H
CD45+
MAC-2+
%CD45+ MAC-2+ of cells
SOD1/IKK
IKK
I
P50
SOD1/IKK
CD11b MAC-2 DAPI
J
CD11b+
MAC-2+
% of CD11b+ MAC-2+ of cells
SOD1/IKK
IKK
K
TMEM119+
86.5%
CD45high
34.6%
MAC-2+
20.43%
Macrophage-like
M ϕ
CD206+
MAC-2-
14.16%
Reactive
Microglia
Mi ϕ
CD45low
51.9%
MAC-2-
Resting
Microglia
IBA1+/ CD11b+
F4/80bright
<5%
Perivascular Mϕ
TMEM119-
13.5%
CD45+/MAC-2-
2.20%
Lymphocytes
< 10%
L
P50
SOD1/IKK
CD11b CD11c DAPI
M
CD11b+
CD11c+
% CD11b+ CD11c+ cells
SOD1/IKK
IKK
N
P50
SOD1/IKK
TMEM119 CD11c DAPI
O
CD11c+
TMEM119+
% TMEM119+ CD11c+ cells
SOD1/IKK
IKK
P
P50
SOD1/IKK
Tmem119 CD11c CD169 DAPI
Q
CD11c+
CD169+
% CD11c+ CD169+ cells
SOD1/IKK
IKK
R
CD169+
TMEM119+
% CD169+ TMEM119+ cells
SOD1/IKK
IKK
S
CD11c+ cells /10⁴ µm²
10
5
2.5
P50
P90
Time (days)

Figure EV1.

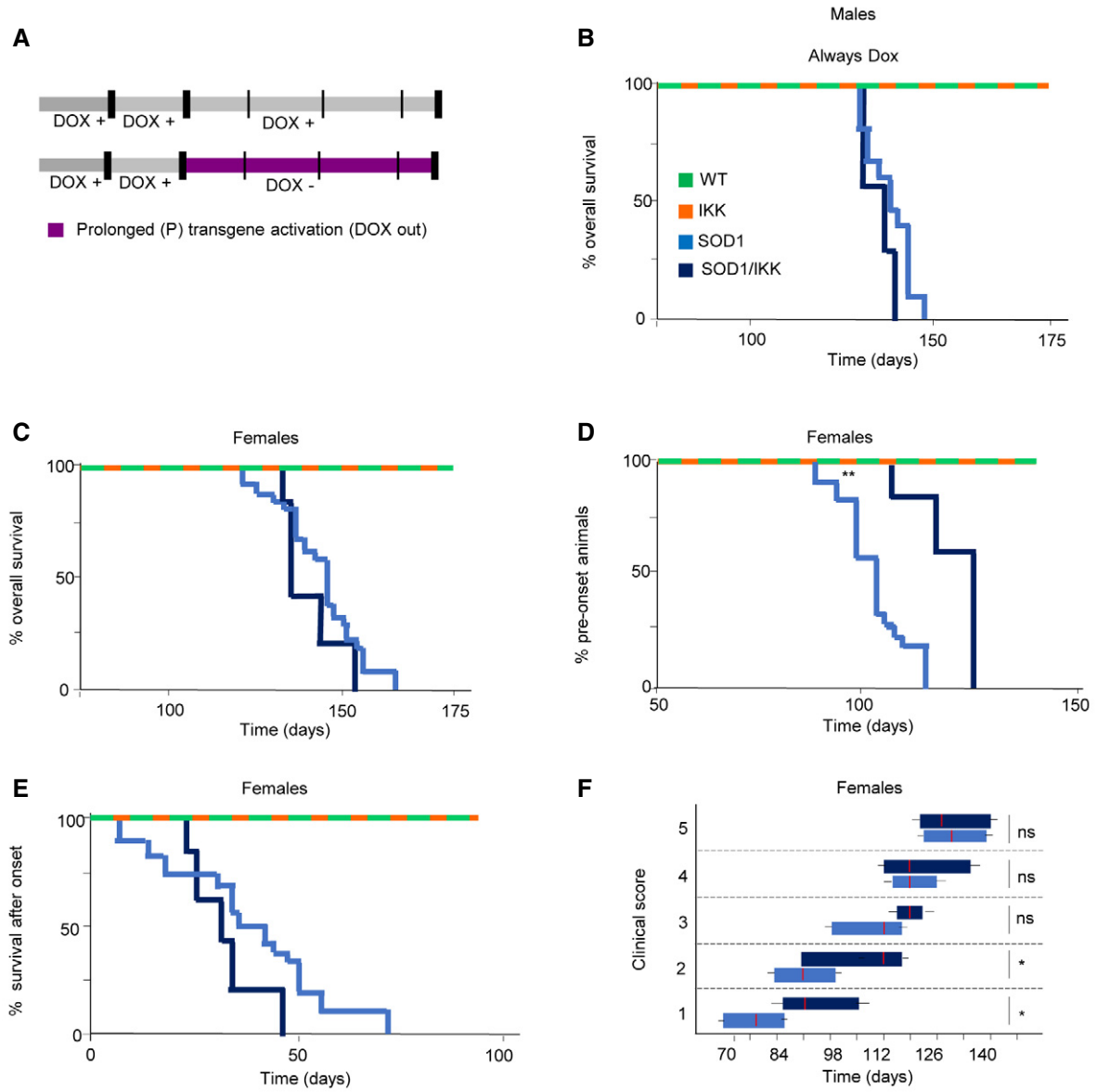

Figure EV2. Time-dependent NF-κB activation in astrocytes differentially affects disease onset and progression.

A Experimental design illustrating no transgene activation (male mice in panel B) or prolonged transgene activation (female mice in panels C–F) induced by DOX withdrawal (DOX out, purple).

B Kaplan–Meier curves of overall survival (% of alive mice over time) of male mice treated with DOX at all time, resulting in inhibition of IKK2-CA transgene expression. No difference between the SOD1 and the SOD1/IKK mice was observed (Mantel–Cox $P = 0.0612$; SOD1 $n = 25$; SOD1/IKK $n = 3$).

C Overall survival depicted in a Kaplan–Meier curve of survival for female mice with prolonged activation. (Mantel–Cox $P = 0.5397$; SOD1 $n = 18$; SOD1/IKK $n = 5$).

D Kaplan–Meier curves representing percentage of female animals in the presymptomatic phase of ALS disease (based on peak weight); (Mantel–Cox $^{**}P = 0.0048$).

E Kaplan–Meier curves representing duration of the progression phase in female mice (Mantel–Cox $P = 0.2266$; SOD1 $n = 18$; SOD1/IKK $n = 5$).

F Time course of the neurological score progression, showing delayed symptoms onset in female SOD1/IKK mice. Data are shown as box and whiskers plot: The horizontal red lines in the middle represent median, box limits represent 10% to 90%, while left and right whisker represent min. and max. value range, respectively. Values were calculated by nonparametric Mann–Whitney test. $^{*}P \leq 0.05$; ns = not significant $P > 0.05$. (Mann–Whitney score 1 $^{*}P = 0.0333$; score 2 $^{*}P = 0.0433$).

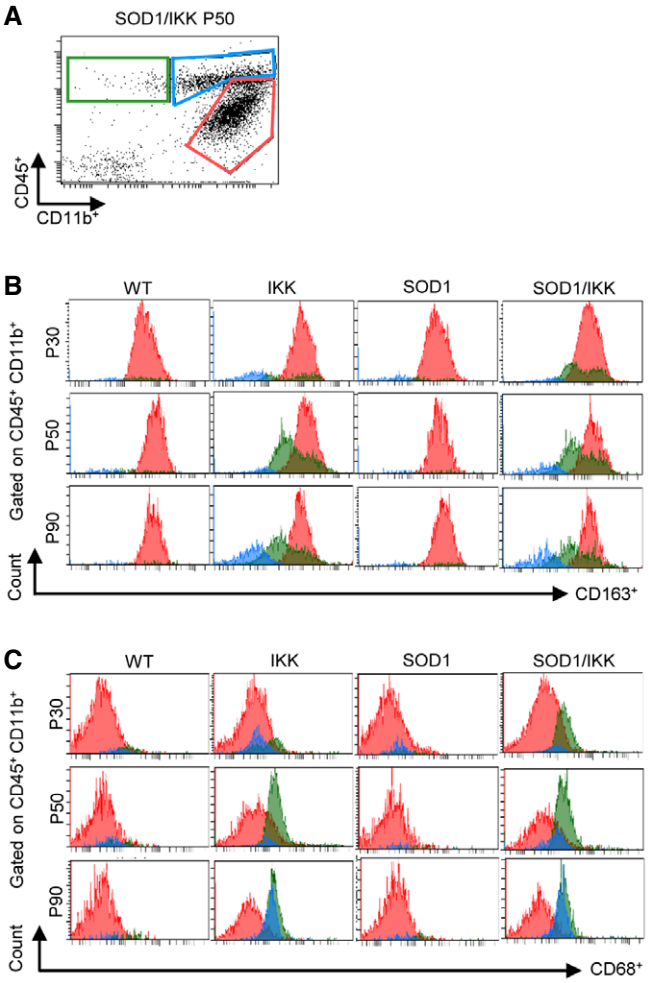

Figure EV3. Microglia immunophenotype characterization after different time points of IKK/NF-κB activation in astrocytes.

A Representative FACS dot-plot of $CD11b^+$ and $CD45^+$ immune cells at P50 on which histograms in (B and C) is gated.

B Histograms of CD163 expression gated on $CD11b^+/CD45^{low\text{-}intermediate}$ (red), $CD11b^+/CD45^+$ (blue), and $CD11b^-/CD45^+$(green) cells at P30, P50, and P90. Distinctive CD163 expression is seen only in $CD11b^+/CD45^{low\text{-}intermediate}$ population and decreases from P30 and P50 to P90.

C Histograms of CD68 expression in $CD11b^+/CD45^{low\text{-}intermediate}$ (red), $CD11b^+/CD45^{high}$ (blue), and $CD11b^-/CD45^+$ (green) subpopulations. Whereas $CD11b^+/CD45^{low\text{-}intermediate}$ express constant low levels of CD68, a strong increase in CD68 expression is detected in $CD11b^+/CD45^{high}$ from P30, P50 to P90.

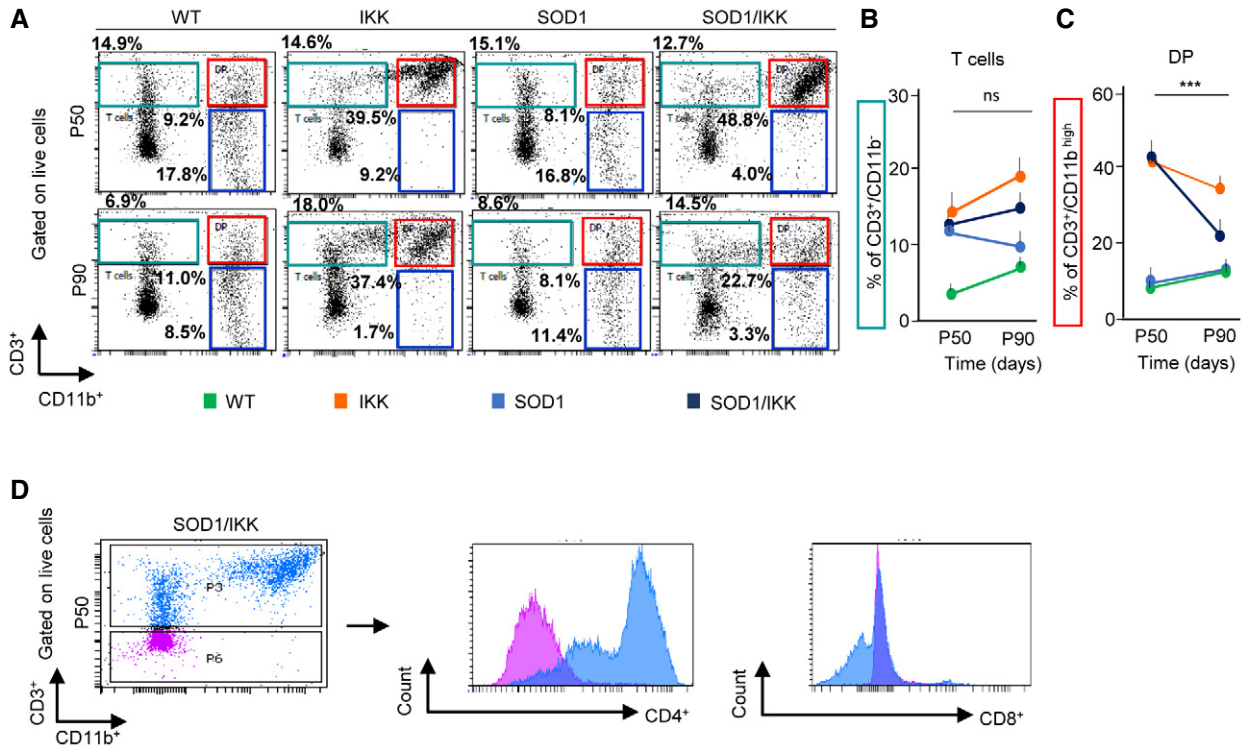

Figure EV4. Characterization of lymphocyte dynamics in lumbar spinal cord in response to NF-κB activation in astrocytes.

A Representative FACS dot-plot showing overall $CD3^+/CD11b^+$ population at P50 and P90 in WT, IKK, SOD1, and SOD1/IKK mice, gated on live cells.

B, C Quantification of (B) $CD3^+CD11b^-$ cells (expressed as %; green in panel A) and (C) $CD3^+/CD11b^{high}$ double-positive populations (DP) (expressed as %; red in panel A) at P50 and P90. P50: WT $n = 4$, IKK $n = 6$, SOD1 $n = 4$, SOD1/IKK $n = 4$; P90: WT $n = 3$, IKK $n = 6$, SOD1 $n = 4$, SOD1/IKK $n = 5$. Two-way ANOVA. Data are shown as means ± SD, $^{***}P \leq 0.001$; ns = not significant, $P > 0.05$.

D FACS dot-plot of $CD3^+/CD11b^+$ population at P50 in SOD1/IKK animal gated on live cells and histograms of $CD4^+$ and $CD8^+$ expression gated on $CD3^{high}$ (blue) and $CD3^{low}$ (purple).

Figure EV5. Wnt signaling is involved in astrocyte-driven microglia expansion after IKK/NF-κB activation in astrocytes.

A Expression of *Wnt1* on mRNA level in spinal cord of P50 mice ($n = 3$–4; relative to HPRT).

B Co-immunostaining of WNT7a (green), GFAP (white), and DAPI (blue) in P50 and P90 animals of all four genotypes.

C Immunostaining for Wnt5a and GFAP in spinal cord from SOD1/IKK mice treated with vehicle or with the PORCN inhibitor C59; Wnt5a immunoreactivity is reduced to < 10% in C59-treated compared to vehicle-treated SOD1/IKK mice (at P38).

D High-magnified representative pictures of $IBA1^+$ staining in IKK and SOD1/IKK animals with either C-59 or vehicle (Veh) treatment from P26 to P38 (early administration).

E Quantification of $IBA1^+$ area in WT, IKK, SOD1, and SOD1/IKK animals with C-59 or Veh treatment from P26 to P38 (% of total area).

F High-magnified representative pictures of $IBA1^+$ staining of IKK and SOD1/IKK, either C-59- or Veh-treated, in late administration between P90 and P102.

G Quantification of $IBA1^+$ cells of C-59- or Veh-treated mice from P90 to P102.

H Quantification of $CD45^+$ cells of IKK and SOD1/IKK animals treated with Veh or C-59 from P90 to P102.

Data information: (E) C59 early treatment: WT $n = 4$, IKK $n = 3$, SOD1 $n = 2$ SOD1/IKK $n = 4$; vehicle-treated: WT $n = 2$, IKK $n = 2$, SOD1 $n = 2$, SOD1/IKK $n = 7$. (G-H) C59 late treatment: WT $n = 2$, IKK $n = 3$, SOD1 $n = 2$ SOD1/IKK $n = 3$; vehicle-treated: WT $n = 3$, IKK $n = 2$, SOD1 $n = 2$, SOD1/IKK $n = 2$. Two-way ANOVA. Data are shown as means ± SD, $^{**}P \leq 0.01$; $^{****}P \leq 0.0001$. Scale bars, 40 μm.

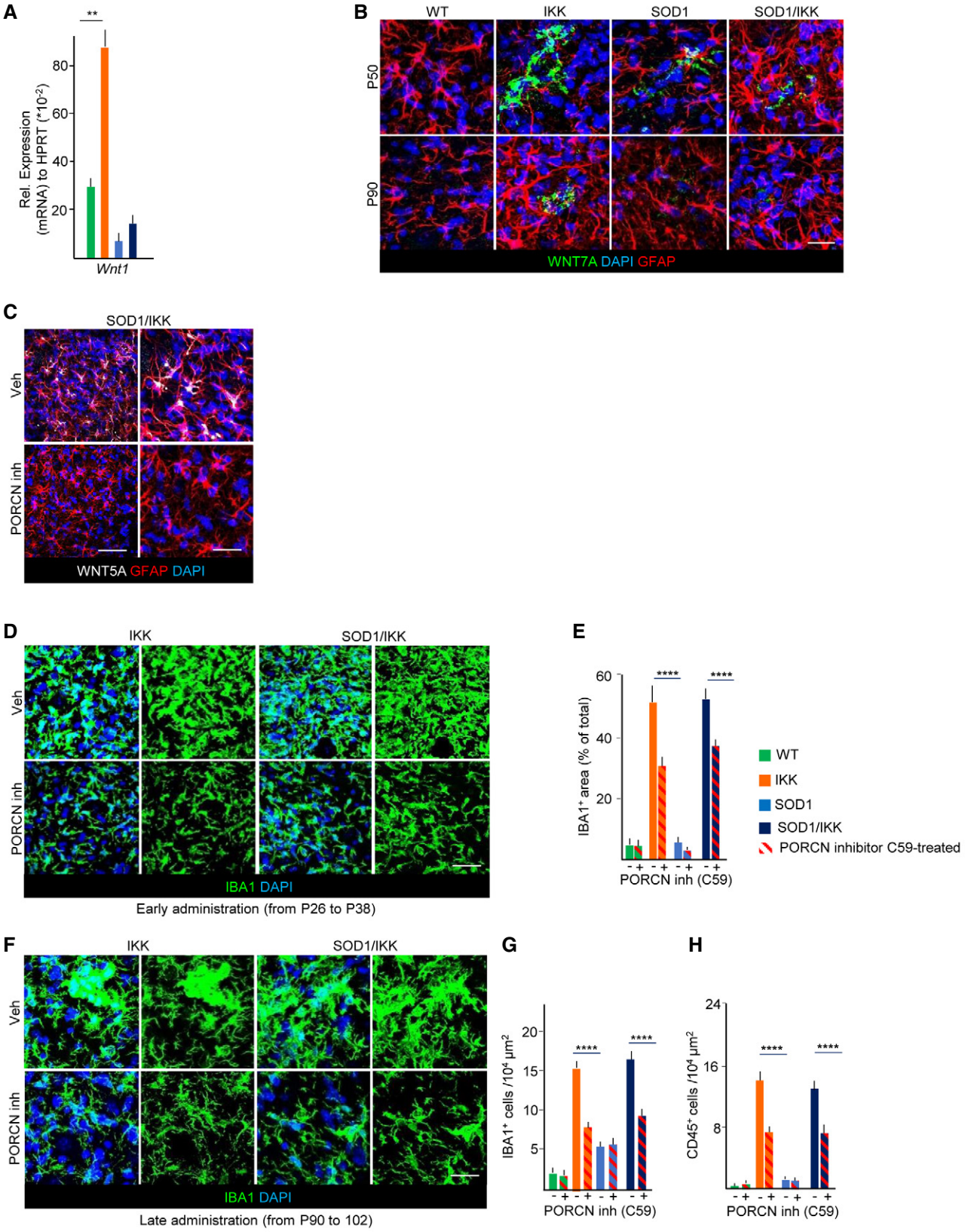
A
**
Rel. Expression (mRNA) to HPRT (*10-2)
80
60
40
20
Wnt1
B
WT
IKK
SOD1
SOD1/IKK
P50
P90
WNT7A DAPI GFAP
C
SOD1/IKK
Veh
PORCN inh
WNT5A GFAP DAPI
D
IKK
SOD1/IKK
Veh
PORCN inh
IBA1 DAPI
Early administration (from P26 to P38)
E
IBA1+ area (% of total)
60
40
20
****
****
- + - + - + - +
PORCN inh (C59)
WT
IKK
SOD1
SOD1/IKK
PORCN inhibitor C59-treated
F
IKK
SOD1/IKK
Veh
PORCN inh
IBA1 DAPI
Late administration (from P90 to 102)
G
IBA1+ cells /10⁴ µm²
20
15
10
5
****
****
- + - + - + - +
PORCN inh (C59)
H
CD45+ cells /10⁴ µm²
24
16
8
****
****
- + - + - + - +
PORCN inh (C59)

Figure EV5.